Theoretical Crack Path Determination

H.A. Richard[1]

[1] Institute of Applied Mechanics, University of Paderborn, Pohlweg 47-49,
33098 Paderborn, Germany, e-mail: richard@fam.upb.de

ABSTRACT. *In many practical cases crack growth leads to abrupt failure of components and structures. For reasons of a reliable quantification of the endangerment due to sudden fracture of a component it therefore is of enormous importance to know the threshold values, the crack paths and the growth rates for the fatigue crack growth as well as the limiting values for the beginning of instable crack growth (fracture toughness). This contribution deals with the complex problem of a – however initiated– crack, that is subjected to a mixed loading. It will present hypotheses and concepts, that describe the superposition of Mode I and Mode II (plane Mixed Mode) as well as the superposition of all three Modes (Mode I, II and III) for spatial loading conditions. Those concepts admit a quantitative appraisal of such crack situations and a characterisation of possible crack paths.*

MIXED MODE FRACTURE AND FATIGUE PROBLEMS

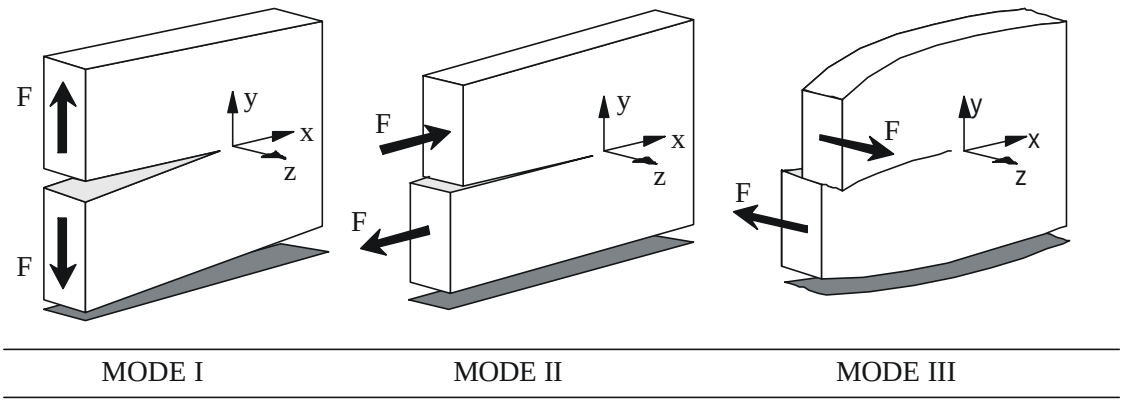

Figure 1. The three fracture modes.

Local Mixed-Mode loading conditions at cracks can be observed, if due to either the external loading or the orientation of the crack the three basic fracture modes (Figure 1) temporarily or permanently occur in combination. This means, that the loading of the structure creates a non-symmetrical, singular stress field in the vicinity of the crack front. Thereby the crack deforms in a way, that not only an opening, but also a planar or non-planar displacement of the two crack surfaces can be found. Consequently the stress field in the vicinity of the crack front is defined not only by the stress intensity

factor K_I, but also by K_{II} and/or K_{III}. In practical cases such crack problems occur e.g. under superimposed loading of a structure, kinked or branched cracks, multiple cracks, cracks initiating from notches, cracks in welded or adhesive joints and in composites. They are caused by static, dynamic or thermic loads, by superposition of load-, thermo- and residual stresses as well as by change of loading or utilisation. Examples for Mixed Mode cracks in a framework can be gather from Figure 2.

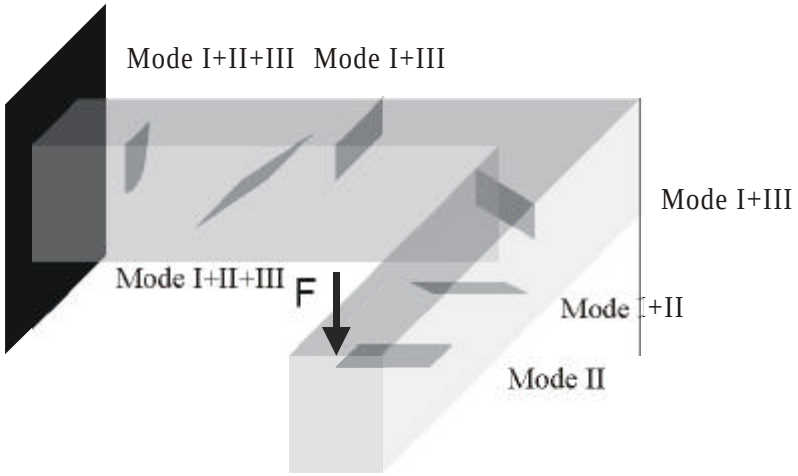

Figure 2. Examples for Mixed Mode crack cases in a frame structure.

The influence of changes in loading and utilisation conditions of a machine part or component is exemplified in Figure 3. Any alteration of the loading condition of the structure might result in an alteration of the crack orientation and the crack path also. The change of the crack growth direction is provoked by a change of the Mixed Mode portions, because in isotropic materials a "long crack" (from a fracture mechanical point of view) only under pure Mode I loading growth straight on (see Figure 4). Mode II loading generally leads to a kinking of crack while Mode III causes a twisting of the crack front. But also the superposition of Mode I, II and III creates special crack surface, which can often be observed in practical cases.

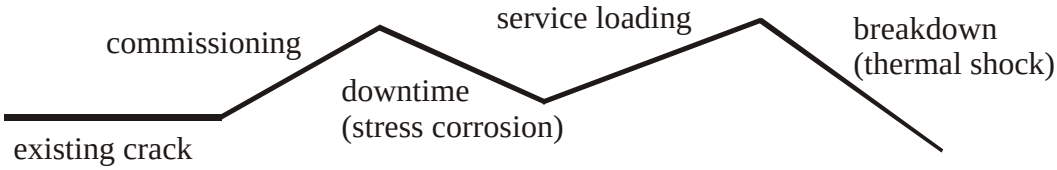

Figure 3. Possible crack propagation during lifetime of a structure.

The superposition of Mode I and Mode II at a crack generally is called *plane Mixed Mode*, while the superposition of all three Modes I, II, III can be characterised as *spatial Mixed Mode* loading condition. Hypotheses and concepts for both plane and spatial Mixed Mode problems will be described in the following.

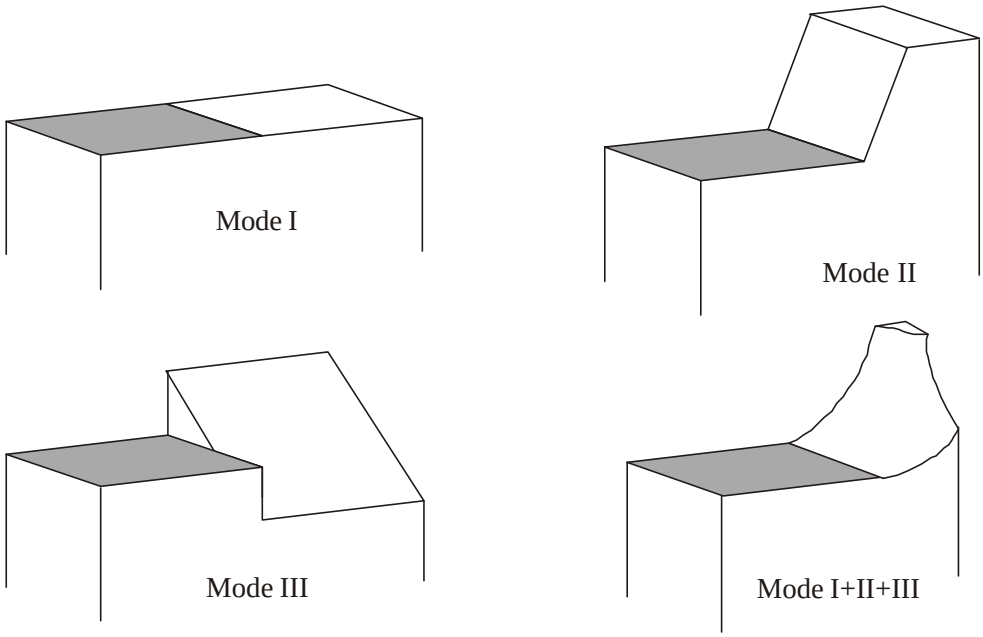

Figure 4. Different types of crack growth under Mixed Mode loading.

The basis for all concepts are the near-field-solution for the stress distribution at the crack front:

$$\sigma_r = \frac{K_I}{4\sqrt{2\pi r}}\left\{5\cos\left(\frac{\varphi}{2}\right)-\cos\left(\frac{3\varphi}{2}\right)\right\}-\frac{K_{II}}{4\sqrt{2\pi r}}\left\{5\sin\left(\frac{\varphi}{2}\right)-3\sin\left(\frac{3\varphi}{2}\right)\right\} \quad (1a)$$

$$\sigma_\varphi = \frac{K_I}{4\sqrt{2\pi r}}\left\{3\cos\left(\frac{\varphi}{2}\right)+\cos\left(\frac{3\varphi}{2}\right)\right\}-\frac{K_{II}}{4\sqrt{2\pi r}}\left\{3\sin\left(\frac{\varphi}{2}\right)+3\sin\left(\frac{3\varphi}{2}\right)\right\} \quad (1b)$$

$$\tau_{r\varphi} = \frac{K_I}{4\sqrt{2\pi r}}\left\{\sin\left(\frac{\varphi}{2}\right)+\sin\left(\frac{3\varphi}{2}\right)\right\}+\frac{K_{II}}{4\sqrt{2\pi r}}\left\{\cos\left(\frac{\varphi}{2}\right)-3\cos\left(\frac{3\varphi}{2}\right)\right\} \quad (1c)$$

$$\tau_{rz} = \frac{K_{III}}{\sqrt{2\pi r}}\sin\left(\frac{\varphi}{2}\right) \quad (1d)$$

$$\tau_{\varphi z} = \frac{K_{III}}{\sqrt{2\pi r}}\cos\left(\frac{\varphi}{2}\right) \quad (1e)$$

$$\sigma_z = \nu(\sigma_r+\sigma_\varphi) = \frac{8\nu}{4\sqrt{2\pi r}}\left\{K_I\cos\left(\frac{\varphi}{2}\right)-K_{II}\sin\left(\frac{\varphi}{2}\right)\right\} \quad (1f)$$

Eqs 1a-1c are valid for plane stress, while Eqs 1d-1fg have to be added for a spatial stress state. All those stress field equations are based in a cylindrical co-ordinate system with the co-ordinates r, φ and z (Figure 5). For $r\rightarrow 0$ all stress fields become singular. The parameters K_I, K_{II} and K_{III} are the stress intensity factors for the three fracture modes (Figure 1). They describe the loading situation at the crack tip and can be used to estimate the risk of fracture as well as for the description of the fatigue crack growth.

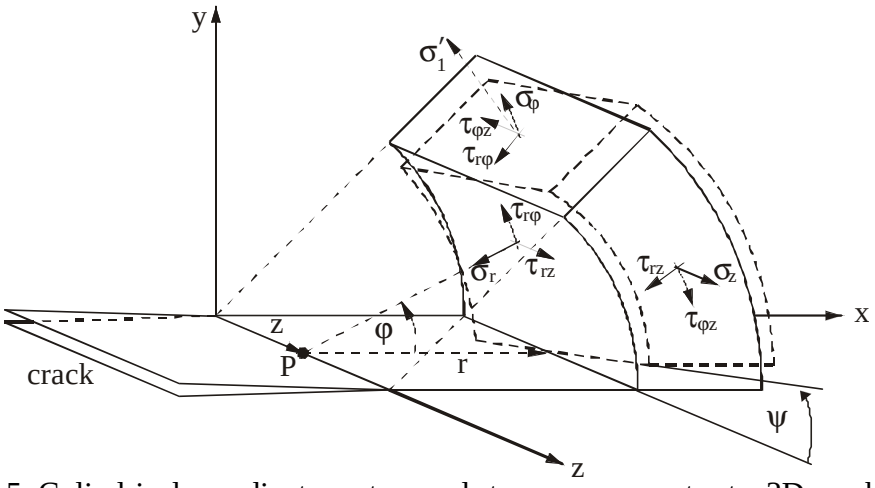

Figure 5. Cylindrical coordinate system and stress components at a 3D crack front.

PLANE MIXED MODE CRACK PROBLEMS

Plane Mixed Mode problems are characterised by the superposition of the fracture modes I and II. Within the scope of the linear elastic fracture mechanics (i.e. the dimensions of the plastic zone around the crack is small in comparison to the crack length and the other dimensions of the structure) the stress field at the crack tip is determined by the intensity factors K_I and K_{II}. Crack growth can take place in stable as well as unstable manner.

Fracture Criteria for Unstable Crack Growth

In the context of unstable crack growth especially the following questions are of interest:

- When does the crack growth become unstable?
- To which direction does the unstable crack grow?
- At what loading level or at what crack length does a structure fail?
- What is the magnitude of safety vs. unstable crack growth/fracture in a structure?

Those questions can be answered by so-called fracture criteria for plane Mixed Mode problems. The most important concepts will be explained in the following.

For pure Mode I loading unstable crack growth occurs, if the Mode I stress intensity K_I reaches the fracture toughness K_{Ic}:

$$K_I \le K_{Ic} \tag{2}$$

The application of this criterion to a Mixed Mode situation would result in a non-conservative estimation for the risk of fracture. For a plane Mixed Mode loading of a crack besides the stress intensity factor K_I also the stress intensity factor K_{II} has an influence on the beginning of unstable crack growth and thus on the fracture of components and structures.

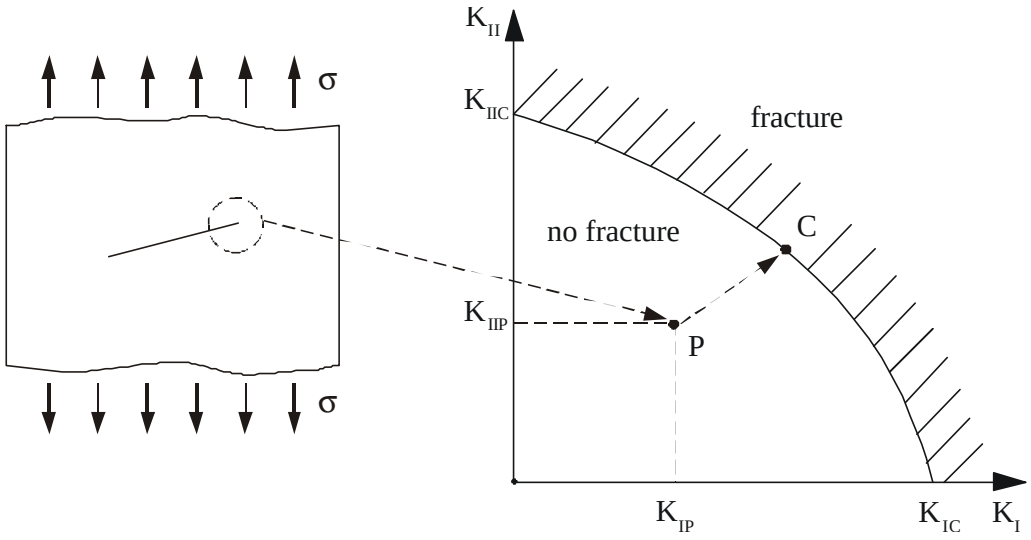

Figure 6. Fracture limit curve for plane Mixed Mode.

As can be seen in Figure 6, the beginning of unstable crack growth can be described by a fracture limit curve. The fracture toughness K_{Ic} then is the limiting value on the K_I-axis. The limit K_{IIc} on the Mode II-axis so far has only very rarely been experimentally determined. If the loading condition at a crack in a structure corresponds to the point P of Figure 6, so no unstable crack growth is to be expected. If in contrast to this the load level increases in a way, that e.g. point C of the fracture limit curve is reached, immediate instable crack growth will occur. In the latter case, the crack kinks according to the K_I- and K_{II}-portions (see Figure 4). Thereby a positive shear stress produces a positive K_{II}-factor, but a negative crack deflection angle $-\varphi_0$, while a negative shear stress results in a negative K_{II} and a positive angle φ_0 (Figure 7).

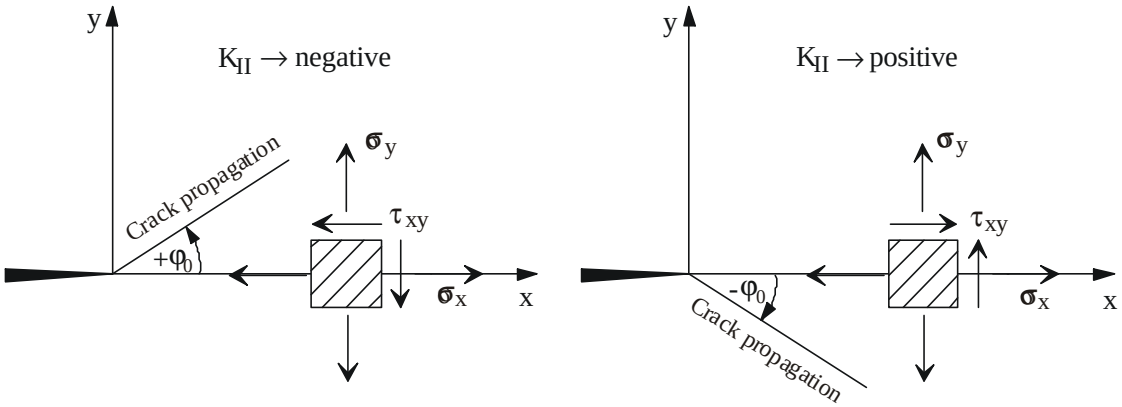

Figure 7. Crack deflection angle under Mixed Mode loading.

The beginning of unstable crack growth as well as the crack growth direction can be determined by the use of one of the following fracture criteria.

Criterion by Erdogan and Sih

The predictions of the maximum tangential stress criterion by Erdogan and Sih [1] are based on the tangential stress σ_φ, Eq. 1b. According to this criterion, the crack growth starts radial from the crack tip with an angle $\varphi=\varphi_0$ perpendicular to the maximum tangential stress $\sigma_{\varphi,max}$. The crack becomes unstable as soon as $\sigma_{\varphi,max}$ exceeds the material limiting value $\sigma_{\varphi,c}$, or –equivalently– if the comparative stress intensity factor K_v resulting from $\sigma_{\varphi,max}$ exceeds the fracture toughness K_{Ic} [2]. The crack deflection angle can be obtained by

$$\left.\frac{\partial\sigma_\varphi}{\partial\varphi}\right|_{\varphi=\varphi_0} = 0 \qquad \text{and} \qquad \left.\frac{\partial^2\sigma_\varphi}{\partial\varphi^2}\right|_{\varphi=\varphi_0} < 0,$$

which yields

$$K_I \sin\varphi_0 + K_{II}(3\cos\varphi_0 - 1) = 0 \tag{3}$$

resp.

$$\varphi_0 = -\arccos\left(\frac{3K_{II}^2 + K_I\sqrt{K_I^2+8K_{II}^2}}{K_I^2+9K_{II}^2}\right) \tag{4}$$

The fracture limit surface is given by

$$K_v = \cos\frac{\varphi_0}{2}\left[K_I\cos^2\frac{\varphi_0}{2} - \frac{3}{2}K_{II}\sin\varphi_0\right] = K_{Ic} \tag{5}$$

Criterion by Sih

The criterion of strain energy density [3] is based on the elastic energy density and the near-field equations for plane Mixed Mode problems. According to this criterion a crack extends –beginning from the crack tip– in the direction of the smallest energy density factor S_{min}. A crack becomes unstable, if S_{min} reaches a material limiting value $S_{min,c}$. Results of this criterion i.a. are presented in [2].

Criterion by Nuismer

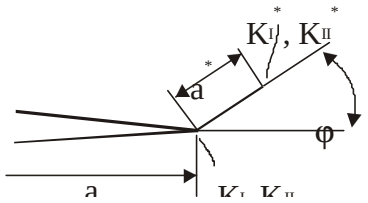

Figure 8. Co-ordinates and stress intensity factors for a kinked crack.

The criterion of energy release rates by Nuismer [4] is based on the assumption of a short kinked crack (Figure 8). For the tip of the kinked crack stress intensity factors K_I^* and K_{II}^* and the energy release rate

$$G(\varphi) = \frac{1-\nu^2}{E}\left(K_I^{*2} + K_{II}^{*\,2}\right) \tag{6}$$

are calculated. According to this criterion the crack propagates into the direction of the maximum energy release rate. Unstable crack growth occurs, if $G_{max}=G_{Ic}$. The results for the crack deflection angles and the fracture limit curve are identical with those of the criterion of maximum tangential stress [2].

Criterion by Amestoy et al.

In the criterion of energy release rates by Amestoy et al. [5] at first for a short branch of a crack the stress intensity factors $\overline{K}_I$ and $\overline{K}_{II}$ and out of it the energy release rate $G(\varphi)$ are calculated. According to this criterion the crack propagates into a direction φ_0, so that $\overline{K}_{II}=0$. Unstable crack growth will occur, if $G(\varphi_0)=G_{Ic}$. The crack deflection angles and the fracture limit curve have to be determined iteratively by this criterion , which i.a. is described in [2].

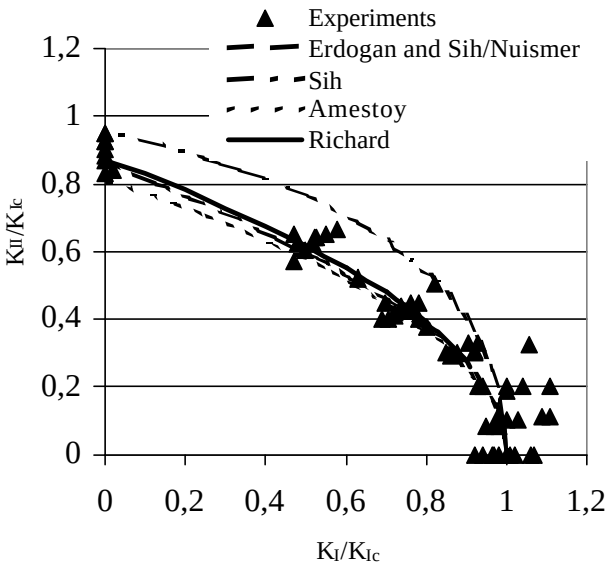

Figure 9. Comparison of the fracture limit curves for different hypotheses with experimental data.

Criterion by Richard

In the generalised fracture criterion [2, 6] a comparative stress intensity factor K_v is defined –comparable to the comparative stress σ_v in the classical stress hypotheses– which depends on the stress intensity factors K_I and K_{II}:

$$K_v = \frac{K_I}{2} + \frac{1}{2}\sqrt{K_I^2 + 4(\alpha_1 K_{II})^2} \le K_{Ic} \qquad (7)$$

Consequently unstable crack growth occurs, as soon as K_v exceeds the fracture toughness K_{Ic} for Mode I. If the material parameter α_1 is set to 1.155, one obtains an excellent approximation of the fracture limit curve of the maximum tangential stress

criterion. For the determination of the crack deflection angle φ_0 there does exist a simple relation, which has been proven by a large number of experiments [2, 7]:

$$\varphi_0 = \mp\left[155{,}5° \frac{|K_{II}|}{|K_I|+|K_{II}|}\right] - 83{,}4° \left[\frac{|K_{II}|}{|K_I|+|K_{II}|}\right]^2, \tag{8}$$

whereby for $K_{II}>0$ the angle $\varphi_0<0$ and vice versa, while always $K_I>0$.

Comparison of the fracture criteria

Figure 9 shows the fracture limit curves resulting from the described criteria. It becomes apparent, that the criteria by *Erdogan/Sih*, *Nuismer* and *Richard* are in good agreement with the experimental findings. Furthermore these criteria are able to predict the crack deflection angle for isotropic and nearly isotropic material sufficiently exact [2].

Fatigue Crack Growth

If a structure is subjected to an oscillating load, even a load level far below the fracture limit might cause a crack to grow under certain circumstances. Thus the following questions arise for plane Mixed Mode fatigue loading:

- Under what conditions does a crack grow?
- Whereto does the crack grow?
- How fast does the crack grow?
- What is the remaining lifetime of the structure?

Fatigue crack growth in plane Mixed Mode loading cases can be observed in the range

$$\Delta K_{I,th} < \Delta K_v < \Delta K_{I,c} \tag{9}$$

This means, that fatigue crack growth is possible, if the cyclic stress intensity factor

$$\Delta K_v = \frac{\Delta K_I}{2} + \frac{1}{2}\sqrt{\Delta K_I^2 + 4(\alpha_1 \Delta K_{II})^2} \tag{10}$$

exceeds the Threshold value $\Delta K_{I,\,th}=\Delta K_{th}$ and is smaller than $\Delta K_{I,c}=(1\text{-}R)K_c$. Generally in this Eq. the parameter α_1 can be set as 1.155. Also in the case of fatigue crack growth the crack generally shows the same sharp kinking as in the static case. For the determination of the kinking angle φ_0 Eq. 8 can be applied.

A very elegant means for the determination of the crack development as well as for the current crack growth rate and remaining lifetime is given by the Finite Element method. In this context especially the program FRANC/FAM [8] is an excellent tool, as it is able to simulate crack growth in planar structures.

THREE-DIMENSIONAL MIXED MODE CRACK PROBLEMS

Spatial Mixed Mode problems are characterised by the superposition of the fracture modes I, II and III. This means, that within the scope of linear-elastic fracture mechanics the stress intensity factors K_I, K_{II} and K_{III} are of importance for the estimation of risk of fracture in structures as well as for the evaluation of stable crack

propagation processes. Depending on the Mode II- and Mode III-portions a more or less intense crack deflection can be observed (Figure 10).

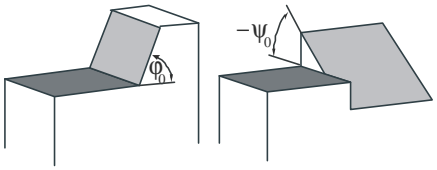

Figure 10. Definition of crack deflection angles φ_0 and ψ_0.

Fracture Criteria for Unstable Crack Growth

For 3D-Mixed Mode problems only very few fracture criteria do exist. The important ones will be described in the following.

Criterion by Sih

At first sight, the well-known Strain Energy Density Criterion by Sih [3, 9] seems to be able to handle three-dimensional crack growth by taking the stress intensity factors K_I, K_{II} and K_{III} that are related to the three fracture modes into consideration. The strain energy density factor is defined as follows:

$$S = a_{11}K_I^2 + 2a_{12}K_I K_{II} + a_{22}K_{II}^2 + a_{33}K_{III}^2 \tag{11}$$

with

$$\begin{aligned}
a_{11} &= \frac{1}{16\pi\mu\cos\psi}\{\ (3-4\nu-\cos\varphi)(1+\cos\varphi)\ \}\\
a_{12} &= \frac{1}{8\pi\mu\cos\psi}\{\ \sin\varphi(\cos\varphi-1+2\nu)\ \}\\
a_{22} &= \frac{1}{16\pi\mu\cos\psi}\{\ 4(1-\nu)(1-\cos\varphi)+(3\cos\varphi-1)(1+\cos)\ \}\\
a_{33} &= \frac{1}{4\pi\mu\cos\psi}
\end{aligned} \tag{12}$$

where μ is the shear modulus of elasticity and ν the Poisson's ratio. The crack angles φ_0 and ψ_0 are derived by minimising S of Eq. (11):

$$\left.\frac{\partial S}{\partial\varphi}\right|_{\varphi=\varphi_0} = 0 \qquad \text{and} \qquad \left.\frac{\partial S}{\partial\psi}\right|_{\psi=\psi_0} = 0 \tag{13}$$

The formulation of φ_0 resulting from the partial derivative of S by φ is depending on Mode-I and Mode-II stress intensity factors and ν but independent of ψ_0 as well as K_{III}. With respect to the second crack deflection angle the minimum of S is given while maximising the term $\cos(\psi_0)$. Therefore, the minimum of S is always in the direction of "ψ=0 –plane" independently of the Mixed-Mode combination. Therefore, this criterion has to be regarded as insensitive to Mode-III. A similar observation can be found in [13].

Criterion by Pook

The second criterion for three-dimensional crack growth that is discussed here is proposed by Pook [10-12]. Pook uses two crack deflection angles φ_0 and ψ_0 (see Figure 10) for the description of the growing crack. For the determination of these angles the equations

$$K_I \sin\varphi_0 = K_{II}(3\cos\varphi_0 - 1) \tag{14}$$

and

$$\tan 2\psi_0 = \frac{2K_{III}}{K_{vI,II}(1-2\nu)} \tag{15}$$

are given resulting in a range of [-70.5°;+70.5°] for φ_0 and [-45°;+45°] for ψ_0. For a Mixed-Mode (I+II+III) loaded crack front Pook's criterion proposes the following strategy. With respect to crack growth predictions the crack deflection angle φ_0 is calculated first using Eq. 14. Afterwards, the comparative stress intensity factors $K_{vI,II}$ and $K_{vI,II,III}$ are determined in a somewhat step-by-step process where the two stress intensity factors K_I and K_{II} for Mode-I and Mode-II define the comparative stress intensity factor $K_{vI,II}$ respectively,

$$K_{vI,II} = \frac{0{,}83K_I + \sqrt{0{,}4489K_I^2 + 3K_{II}^2}}{1{,}5} \tag{16}$$

which is then considered for the calculation of $K_{vI,II,III}$ as defined in Eq. (17):

$$K_{vI,II,III} = \frac{K_{vI,II}(1+2\nu) + \sqrt{K_{vI,II}^2(1-2\nu)^2 + 4K_{III}^2}}{2} = K_{Ic} \tag{17}$$

Finally, ψ_0 results from Eq. 15.

Criterion by Schöllmann et al.

The σ_1'-criterion [14, 15] is based on the assumption that crack growth develops perpendicular to the direction of σ_1' which is a special maximum principal stress. σ_1'can be found on a virtual cylindrical surface whose axis is represented by the regarded part of the crack front. The stress state on the cylindrical surface and the local co-ordinate system of the cylinder is shown in Figure 5, where the z-axis is tangential to the crack front, the y-axis normal and the x-axis binormal to the crack plane.

In the three-dimensional case the crack growth direction is perpendicular to the maximum principal stress σ_1' which is defined by the near-field stresses σ_φ, σ_z and $\tau_{\varphi z}$ as follows:

$$\sigma_1' = \frac{\sigma_\varphi + \sigma_z}{2} + \frac{1}{2}\sqrt{(\sigma_\varphi - \sigma_z)^2 + 4\tau_{\varphi z}} \tag{18}$$

Due to the assumption, that the crack growth direction is perpendicular to σ_1', the crack deflection angle φ_0 as defined in Figure 10 can be calculated:

$$\left.\frac{\partial\sigma_1'}{\partial\varphi}\right|_{\varphi=\varphi_0} = 0 \qquad \text{and} \qquad \left.\frac{\partial\sigma_1'}{\partial\varphi}\right|_{\varphi=\varphi_0} < 0 \tag{19}$$

After substituting the near-field solutions of Eq. 1 into Eq. 19, considering $\sigma_z=0$ and differentiating partially by φ_0 the following formulation can be found for φ_0:

$$-6K_I\tan\left(\frac{\varphi_0}{2}\right)-K_{II}\left(6-12\tan^2\left(\frac{\varphi_0}{2}\right)\right)+\left\{\left[4K_I-12K_{II}\tan\left(\frac{\varphi_0}{2}\right)\right]\cdot\right.$$
$$\cdot\left[-6K_I\tan\left(\frac{\varphi_0}{2}\right)-K_{II}\left(6-12\tan^2\left(\frac{\varphi_0}{2}\right)\right)\right]-32K_{III}^2\tan\left(\frac{\varphi_0}{2}\right)\cdot \quad (20)$$
$$\left.\cdot\left(1+\tan^2\left(\frac{\varphi_0}{2}\right)\right)^2\right\}\cdot\left\{\left[4K_I-12K_{II}\tan\left(\frac{\varphi_0}{2}\right)\right]^2+64K_{III}^2\left(1+\tan^2\left(\frac{\varphi_0}{2}\right)\right)^2\right\}^{-1/2}=0$$

The second deflection angle ψ_0 (Figure 10) is defined by the direction of σ_1' and can be calculated according to the calculation of the maximum principal stress angle using Eq. 21:

$$\psi_0=\frac{1}{2}\arctan\left(\frac{2\tau_{\varphi z}(\varphi_0)}{\sigma_\varphi(\varphi_0)-\sigma_z(\varphi_0)}\right) \quad (21)$$

During the investigation of fatigue cracks under superimposed normal and shear loading the determination of a comparative stress intensity factor K_v is necessary for the calculation of the portion of crack propagation. For plane loading conditions K_v is only depending on K_I and K_{II}. Dealing with three-dimensional crack fronts K_{III} has to be taken into consideration as well. From Eq. 18 a formulation for K_v can be derived as follows:

$$K_v=\frac{1}{2}\cos\left(\frac{\varphi_0}{2}\right)\left\{K_I\cos^2\left(\frac{\varphi_0}{2}\right)-\frac{3}{2}K_{II}\sin(\varphi_0)\right.$$
$$\left.+\sqrt{\left[K_I\cos^2\left(\frac{\varphi_0}{2}\right)-\frac{3}{2}K_{II}\sin(\varphi_0)\right]^2+4K_{III}^2}\right\}=K_{Ic} \quad (22)$$

where K_{Ic} is the fracture toughness for pure Mode I-loading.

Criterion by Richard

In order to simplify the prediction of crack growth under multiaxial loading approximation functions have been developed [7]. Furthermore, the formulas are helpful for practical application.

The function Eq. 8 can easily be extended for Mixed-Mode I+II+III loading conditions by replacing the denominator ($K_I+|K_{II}|$) by ($K_I+|K_{II}|+|K_{III}|$). This leads to the new approximation function for the crack deflection angle φ_0 as defined in Figure 10:

$$\varphi_0=\mp\left[A\frac{|K_{II}|}{K_I+|K_{II}|+|K_{III}|}+B\left(\frac{|K_{II}|}{K_I+|K_{II}|+|K_{III}|}\right)^2\right] \quad (23)$$

where $\varphi_0<0°$ for $K_{II}>0$ and $\varphi_0>0°$for $K_{II}<0$ and $K_I \geq 0$.

For the calculation of the second crack deflection angle ψ_0 this approach is applicable as well. The new approximation function for ψ_0 (Figure 10)is given in Eq. (24):

$$\psi_0 = \mp\left[C\frac{|K_{III}|}{K_I + |K_{II}| + |K_{III}|} + D\left(\frac{|K_{III}|}{K_I + |K_{II}| + |K_{III}|}\right)^2 \right] \tag{24}$$

where $\psi_0<0°$ for $K_{III}>0$ and $\psi_0>0°$ for $K_{III}<0$ and $K_I \geq 0$.

With A=140°, B=-70°, C=78° and D=-33° the Eqs 23 and 24 are in good agreement with the crack deflection angles predicted by the σ_1'-criterion.

Unstable crack growth will occur if the local loading condition along the crack front reaches a point on the fracture limit surface (Figure 14). This situation can be described by the following fracture criterion [7]:

$$K_v = \frac{K_I}{2} + \frac{1}{2}\sqrt{K_I^2 + 4(\alpha_1 K_{II})^2 + 4(\alpha_2 K_{III})^2} = K_{Ic} \tag{25}$$

where $\alpha_1=K_{Ic}/K_{IIc}$ and $\alpha_2=K_{Ic}/K_{IIIc}$. With $\alpha_1=1.155$ and $\alpha_2=1.0$ Eq. 25 is in excellent agreement with the K_v-prediction of the σ_1'-criterion, Eq. 22.

Comparison of the Fracture Criteria

All of the proposed fracture criteria yield predictions concerning the crack deflection angles φ_0 and ψ_0 and the fracture limit surface for the superposition of all three fracture modes. Figure 11 presents a diagram of the crack deflection angle φ_0 according to the criterion of Schöllmann et al. In Figure 12 a diagram for the twisting angle ψ_0 is depicted, which results from the criterion by Pook. Finally the fracture limit surface resulting from the criterion by Richard can be seen in Figure 13. If the loading of the crack reaches this limit, unstable crack growth will immediately occur. A more detailed comparison of the criteria can be found in [17].

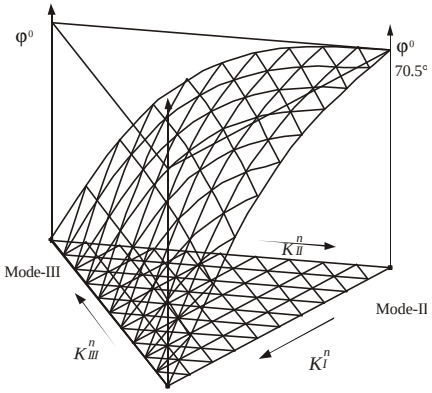

Figure 11. Crack deflection angle φ_0 according to Schöllmann et al.

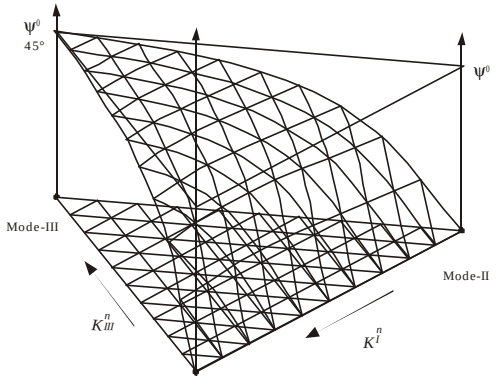

Figure 12. Crack deflection angle ψ_0 according to Pook with ν=0.3.

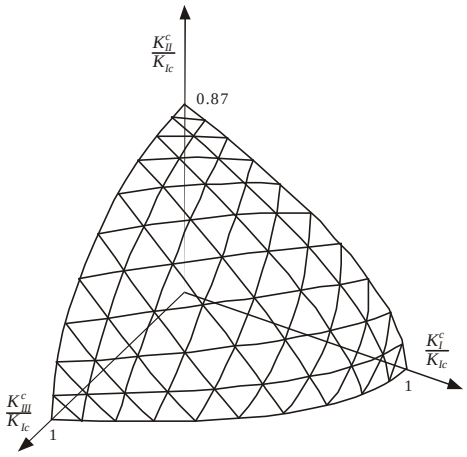

Figure 13. Fracture limit surface according to Richard.

The following Table 1 presents the values for the crack deflection angles and the fracture limit, which results from the proposed criteria for pure Mode I, II and III loading conditions.

Table 1. Results of the 3D criteria.

	Sih	Pook	Schöllmann et.al.	Richard
Mode I:				
φ_0	0°	0°	0°	0°
ψ_0	0°	0°	0°	0°
K_{IC}	K_{IC}	K_{IC}	K_{IC}	K_{IC}
Mode II:				
φ_0	82,3°	70,5°	70,5°	70,5°
ψ_0	0°	0°	0°	0°
K_{IIC}	0,96 K_{IC}	0,87 K_{IC}	0,87 K_{IC}	0,87 K_{IC}
Mode III:				
φ_0	undef.	undef.	0°	0°
ψ_0	0°	45°	45°	45°
K_{IIIC}	0,63 K_{IC}	K_{IC}	K_{IC}	K_{IC}

Fatigue Crack Growth

A crack, which is subjected to an arbitrary Mixed mode loading, is able to propagate under fatigue crack growth conditions, if the local crack front loading combined of Mode I, II and III portions is located in between the Threshold and 3D fracture-surface in the K_I-K_{II}-K_{III}-diagram (Figure 14).

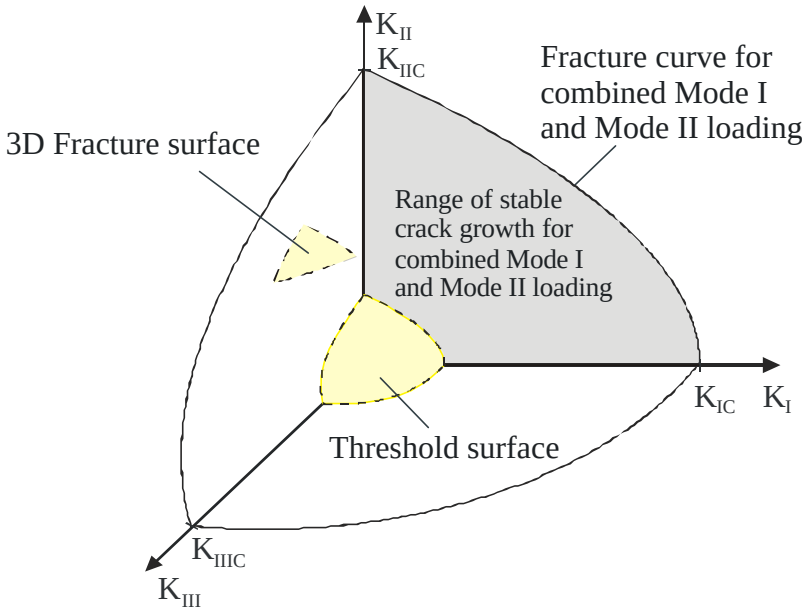

Figure 14. K_I-K_{II}-K_{III}-diagram for Mixed Mode loading with the fracture limit and the Threshold surface.

This condition can be written down by the formula

$$\Delta K_{I,th} < \Delta K_v < \Delta K_{I,c} \tag{26}$$

Hereby ΔK_v is the cyclic comparative stress intensity factor, which can be derived from Eq. 25:

$$\Delta K_v = \frac{\Delta K_I}{2} + \frac{1}{2}\sqrt{\Delta K_I^2 + 4(\alpha_1 \Delta K_{II})^2 + 4(\alpha_2 \Delta K_{III})^2} \tag{27}$$

As before, α_1=1.155 and α_2=1.0.

For 3D- Mixed Mode problems crack growth simulations can be performed also by the means of the Finite Element method. I.a. the program system ADAPCRACK3D is a valuable tools for such kind of simulations [18, 19].

CONCLUSION

For theoretical determination of crack paths and the examination of crack and crack growth problems in real structures several hypotheses and concepts are available. Under consideration of experimental experiences with the brittle fracture behaviour of cracks can be pointed out, that for plane Mixed Mode problems the criteria by *Erdogan/Sih* and *Richard* and for 3D-Mixed Mode Problems the criteria by *Schöllmann et al*. and *Richard* are well suited for the description of crack growth. For the purpose of analysing crack paths and crack propagation processes under fatigue loading in real structures those concepts have to be implemented in Finite-Element programs. Special cases, like

the crack growth in anisotropic materials or the sliding of cracks under pure Mode II or Mode III loading can however not be reasonably described by the proposed concepts.

REFERENCES

1. Erdogan, F., Sih, G.C. (1963) *J. Basic Engng*. **85**, 519-525
2. Richard, H.A. (1985) *Bruchvorhersage bei überlagerter Normal- und Schubbeanspruchung von Rissen*, VDI-Verlag, Düsseldorf.
3. Sih, G.C. (1974) *Int. J. Fract.* **10**, 305-321.
4. Nuismer, R.J. (1975) *Int. J. Fract.* **11**, 245-250.
5. Amestoy, M., Bui, H.D. and Dang Van K. (1980) In: *Advances in Fracture research*, pp. 107-113, Francois, D. et al. (Eds.), Oxford.
6. Richard, H.A. (1987) In: *Structural failure, product liability and technical insurance*, Rossmanith (Ed.), Inderscience Enterprises Ltd., Genf.
7. Richard, H.A. (2001) In: *CD-Rom Proceedings of ICF10*, Honolulu, USA.
8. Schöllmann, M. and Richard, H.A. (1999) *J. Struct. Engng.* **26,** 39-48.
9. Sih, G.C. (1990). *Mechanics of fracture initiation and propagation*, Kluwer Academic publishers, Dodrecht, Netherlands.
10. Pook, L.P. (1980) In: *Fracture and Fatigue: Elasto-Plasticity, Thin Sheet and Micromechanism Problems*, pp. 143-153, Radon, J.C. (Ed.) Pergamon Press, Oxford.
11. Pook, L.P. (1985) *Multiaxial Fatigues*, pp. 249-263 In: Miller, K.J., Brown, M.W. (Eds.), ASTM STP853, American Society for Testing and Materials, Philadelphia.
12. Pook, L.P. (2000) *Linear elastic fracture Mechanics for engineers: theory and application.* WIT press, Southampton.
13. Mi, Y. (1996) *Topics in Engineering*, p. 28 In: Brebbia, C.A., Connor, J. Computational Mechanics Publications, Southampton.
14. Schöllmann, M., Kullmer, G., Fulland, M. and Richard, H.A. (2001) *Proc. of 6th Int. Conf. of Biaxial/Multiaxial Fatigue & Fracture*, Vol. **2**, 589-596.
15. Schöllmann, M., Richard, H.A., Kullmer, G. and Fulland, M. (2002) *Int. J. Fract.* **117**, 129-141.
16. Richard, H.A, Schöllmann, M., Fulland, M. and Sander, M. (2001), *Proc. of 6th Int. Conf. of Biaxial/Multiaxial Fatigue & Fracture*, Vol. **2**, 623-630.
17. Richard, H.A., Schöllmann, M., Buchholz, F.G. and Fulland, M. (2003) In: *DVM-Bericht 235*, pp. 327-339, Deutscher Verband für Materialforschung und –prüfung e.V., Berlin.
18. Schöllmann, M., Fulland, M. and Richard, H.A. (2003) *Engng. Fract. Mech.* **70,** 249-268.
19. Fulland, M. and Richard, H.A. (2003) *Proc. of FCP2003*.